Spring-constant measurement methods for RF-MEMS capacitive switches

Jiahui Wang, Jeroen Bielen, Cora Salm, and Jurriaan Schmitz

***Abstract*: In this article we compare three approaches to measure the spring constant in RF MEMS capacitive switches. We use the lowest vibration mode, as obtained from vibrometry; the pull-in voltage; and the low-field capacitance-voltage curve of the device to extract the spring constant. Experimental results are presented for each approach, and FEM model predictions are used to further verify and interpret the findings. Pros and cons of each method are discussed.**

***Index Terms*—MEMS switch, spring constant, capacitance-voltage measurement, resonance**

I. Introduction

Radio-frequency microelectromechanical (RF MEMS) capacitive switches offer substantial advantages over p-i-n diodes or CMOS transistor switches, such as lower insertion loss, higher isolation, higher linearity and lower power consumption [1,2,3]. Some important parameters of the RF MEMS switches, such as pull-in voltage and resonant frequency, relate with the spring constant (k). The measurement of k is important to characterize the RF MEMS switch; it may be a suitable parameter for in-line process control if a fast and reliable wafer-level electrical measurement is developed. In this article, we discuss three approaches to determine the spring constant. They are tested on four designs of RF MEMS switches, and compared with 3D FEM simulation results of the same devices.

II. Experimental

Figure 1 shows a top view microscope image of the four studied RF MEMS switches. The devices are supplied by EPCOS AG; they were produced in an intermediate stage of process development and intended for reliability characterization. Further documentation of the switches is found in [6]. The switches have various spring designs, with longer springs going from device 0 to device 3. The electrodes are identical in each device. The movable top electrode is a large perforated square (area A=300*300 μm^2). Springs suspend the top electrode over the bottom electrode. A SiN/SiO_x dielectric layer is deposited on the bottom electrode (cf. figure 1, bottom). The signal bond pads are connected to the bottom electrode; ground bond pads to the top electrode. The pads, electrodes and connection lines are aluminum-based. Vertical dimensions

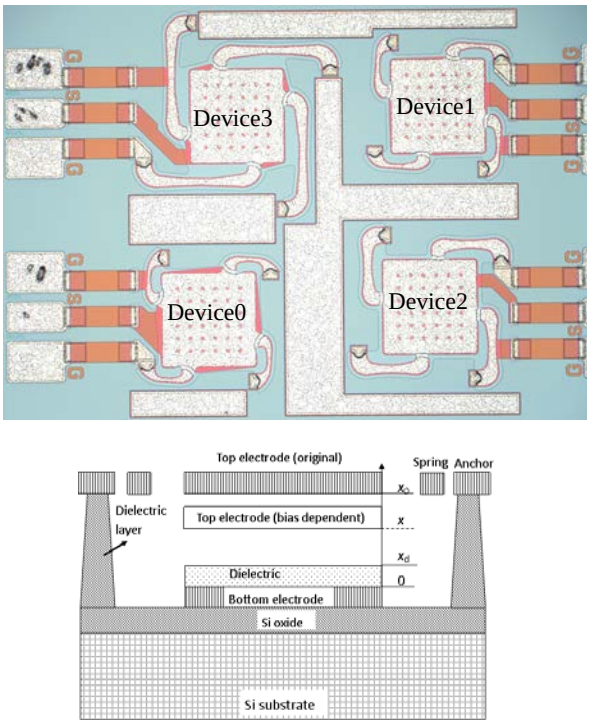

Figure 1: top view microscope image of the RF MEMS capacitive switches under study (top); the bottom sketch shows a schematic cross-sectional view of the RF MEMS capacitive switch. The position of the upper surface of the bottom electrode is defined as height 0. The original height of the top electrode x_0 is around 3 µm; the dielectric layer x_d is around 560 nm with a permittivity ε_r of 7.4; x is the bias dependent height of the top electrode.

of the device are in the caption of figure 1.

An elaborate 3D multi-physics finite-element simulation has been set up to model the capacitance-voltage (C-V) behavior of the switches in ANSYS and validated on data from similar devices as studied in this work [7,8]. The model takes into account fringe field effects, process induced initial stress and stress gradients and uses non-linear plasticity for the metal top electrode. The mechanical behavior is measured by scanning laser Doppler vibrometry. A DC bias and a sinusoidal AC voltage is applied to the MEMS switch; the velocity of the top electrode and the phase between the electrical input and the mechanical output are measured. The mechanical displacement of the top electrode is calculated by velocity integration. Figure 2 shows two typical FEM results, where the vertical deflection of the top electrode and the springs at pull-in is depicted, at pull-in, and under small-signal excitation at the ground resonance frequency.

The C-V curve is measured with a Keithley 4200 CVU at 800 kHz. The short compensation is negligible at 800 kHz.

Jiahui Wang, Cora Salm, and Jurriaan Schmitz are with the MESA+ Institute for Nanotechnology, group Semiconductor Components, University of Twente, 7500 AE Enschede, The Netherlands. E-mail: j.schmitz@utwente.nl; website www.utwente.nl/ewi/sc. Jeroen Bielen is with EPCOS Netherlands B.V., Nijmegen, The Netherlands.

To get an accurate open compensation, we mechanically removed the top electrode of a device to create 'open structures' for each of the four studied switches. Half of the measured impedance of the 'open structure' is used as the open compensation, as further explained in [4]. The same reference also provides further information on calibration, de-embedding and electrical *C-V* measurement as we applied them. In addition to the procedures detailed in that work, each MEMS switch under study is switched twice before characterization, as explained later in this article.

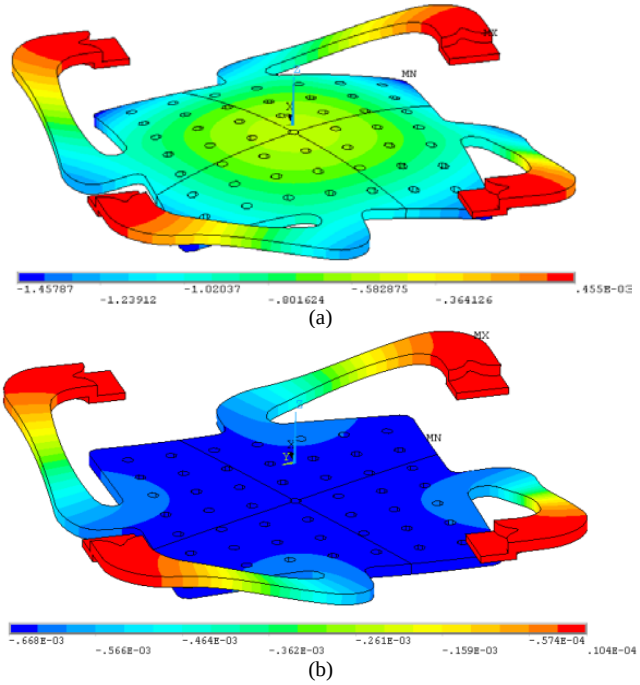

Figure 2: FEM model calculation results: (a) vertical displacement of device 1 at V_{pi}; (b) small signal vertical displacement around bias point of device 1 at the first resonance. The scale bars are in µm.

III. Theory

In this section we will describe three approaches to derive the spring constant from device measurements. It is worth noting that the four springs create one effective spring constant together, but only if the top electrode is rigid and each corner exhibits the same translation. The perforations in the top electrode lead to a slightly distance-dependent capacitance. Altogether, we can expect that different measurement approaches at different bias conditions will yield slightly different spring constant values.

A. Spring constant from vibrometry measurements

A measurement of the resonant behavior of the top electrode under periodic bias can be used to determine the spring constant. Both amplitude and phase depend on the applied frequency. The phase difference between electrical input and the mechanical displacement output equals -90° at the Eigen frequency ω_0 associated with the resonance. The resonance frequency is the frequency at which the maximum displacement of the top electrode occurs. The resonance frequency is close to ω_0 but becomes smaller than ω_0 for damped devices [5]. Therefore, we use the Eigen frequency to calculate k. In the (simplistic) 1-D approximation of a mass-spring system we have:

$$k=\omega_0^2 m = \omega_0^2 \rho A t_{TE} \qquad (1)$$

In this equation, m is the effective mass of the top electrode which is approximated with the mass of the rectangular plate, ρ is its density, A its effective surface area, and t_{TE} is its thickness [9]. We can see from this equation that the accuracy of the mass estimation affects the absolute value of k linearly.

This vibrometry method has the advantage of being independent of the gap size, and insensitive to fringe capacitance; plus it does not require de-embedding. The dedicated measurement set-up can only be used for unpackaged devices.

B. Spring constant from pull-in voltage

The RF-MEMS device will close at a specific DC bias known as the pull-in voltage (V_{pi}) [5]. Assuming that the electrostatic force can be described with a parallel-plate approximation, and that Hooke's law is applicable, we can find the following equation for the equilibrium of the top electrode under DC bias:

$$F_{ext} = \frac{V_{DC}^2 \varepsilon_0 A}{2(g+u)^2} + ku = 0 \qquad (2)$$

where V_{DC} is the DC bias; ε_0 is the vacuum permittivity; $g=x_0-x_d+x_d/\varepsilon_r$ is the effective gap of the parallel-plate capacitance at zero DC bias; $u=x-x_0$ is the vertical displacement of the top electrode from the equilibrium position at zero DC bias; thus $g+u=x-x_d+x_d/\varepsilon_r$ is the bias dependent effective gap of the parallel-plate capacitance. When $g+u=2g/3$, pull-in occurs [5]. Inserting $V_{DC}=V_{pi}$ and $g+u=2g/3$ into equation 2, the spring constant is found as:

$$k = \frac{27\varepsilon_0 A V_{pi}^2}{8g^3} \qquad (3)$$

With the measurement of V_{pi} (for instance, with a high frequency *C-V* measurement), and knowledge of the geometrical parameters, we can thus determine k. As pull-in has a very pronounced signature in the *C-V* curve, V_{pi} determination is easy and accurate, even without calibration and de-embedding. Measurement-induced stress effects may occur using this method, in contrast to the other two.

In the above equation we assume that no dielectric charge is present. A homogeneous dielectric charge would lead to a voltage shift V_s of the entire *C-V* curve. So one may take the average of (the absolute value of) the positive and negative V_{pi} to avoid the influence of dielectric charge. We have further assumed that the fringe capacitance is negligible, i.e. the parallel-plate equation can be used for the capacitance in equation 3. If the fringe capacitance is considered, we can, as first order correction, treat this as an area correction in equation 3. As a result, the determination of k is linearly affected by fringe capacitance errors. Finally, as the top electrode is not rigid and has several degrees of motional freedom, this description may yield inaccurate results.

C. Spring constant from low-field C-V curve

We can also estimate the spring constant from the "sag" of the top electrode when a small DC bias is applied, by measuring its capacitance around 0 V, with a measurement frequency much larger than Eigen frequency. At low-field, $u<<g$, and therefore the parallel-plate capacitance can be

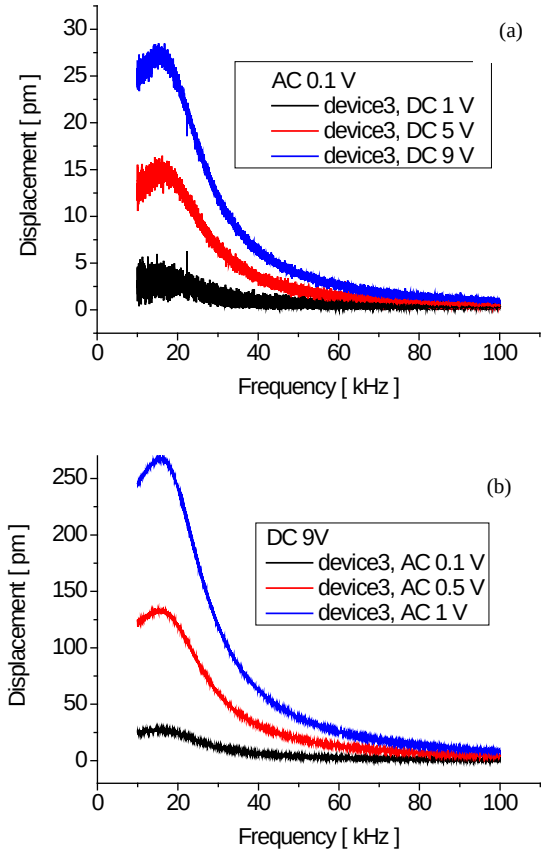

Figure 3: the displacement-frequency curves of device 3 at (a) AC voltage of 0.1 V and various DC biases; and (b) at DC of 9 V and various AC voltages.

approximated as

$$C = \frac{\varepsilon_0 A}{g+u} \approx \frac{\varepsilon_0 A}{g}\left(1 - \frac{u}{g}\right) \qquad (4)$$

From equation 2 follows that

$$u = -\frac{{V_{DC}}^2 \varepsilon_0 A}{2k(g+u)^2} \approx -\frac{{V_{DC}}^2 \varepsilon_0 A}{2kg^2} \qquad (5)$$

Inserting (5) into (4):

$$C = \frac{{\varepsilon_0}^2 A^2}{2kg^4}{V_{DC}}^2 + \frac{\varepsilon_0 A}{g} \qquad (6)$$

So the low-field *C-V* curve can be approximated by a parabola shape: $C=aV_{DC}^2+b$ as was experimentally observed earlier [10]. The minimum capacitance equals *b*. The spring constant can be determined as

$$k = \frac{{\varepsilon_0}^2 A^2}{2g^4 a} \qquad (7)$$

In equation (6), V_{DC} should be replaced by V_{DC}-V_s if homogeneous dielectric charging is considered, while equation 7 remains unaffected. Clearly, when we use this equation we are more sensitive to dimensional errors, given the quadratic dependence on *A* and even a fourth power dependence on *g*.

IV. Results and Discussion

A. Vibrometry

Figure 3 shows the mechanical response of the RF MEMS switches under DC bias as measured by a vibrometer. As shown in figure 3 (a) and (b), the magnitude of displacement of the top electrode increases with DC bias and with AC voltage, consistent with the mechanical displacement *u* leading to higher electrostatic force. The resonant frequency (and Eigen frequency) is independent of both DC bias and AC voltage within the measured range. In principle, the MEMS switch is considered a voltage controlled electrostatic transducer. Its Eigen frequency will reduce when the DC bias approaches the pull-in voltage, reflected in a lower effective spring constant [5]. However, when the DC bias is not close to pull-in voltage, the decrease of Eigen frequency is not significant, and the estimation of spring constant in equation (1) is still accurate.

To obtain low-noise measurement curves, we use a DC bias of 9 V and an AC voltage of 1 V to study the four MEMS switches. The displacement-frequency and phase-frequency curves of the four MEMS switches under study are shown in figure 4(a) and (b). The resonant frequency (where the maximum displacement happens) is slightly smaller than Eigen frequency (where the phase equals to -90˚). It is significantly lower when the springs are longer, as expected.

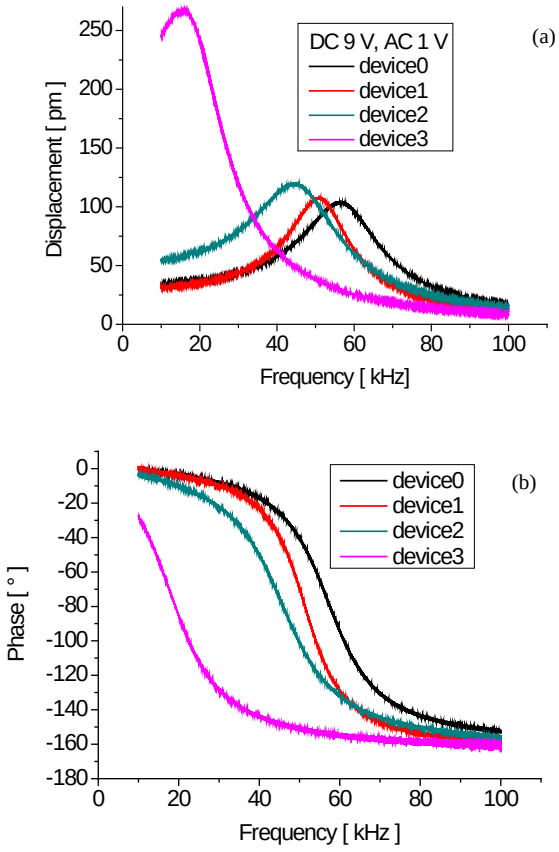

Figure 4: the displacement (a) and phase as a function of frequency of four MEMS switches measured at DC bias of 9 V and AC voltage of 1 V.

The resonances shown in figures 3 and 4 are the first (fundamental) resonance. If we increase the frequency of the AC signal, further resonances will be measured, because the MEMS switch has more than one resonance mode [8,9]. The

spring constant given in equation (1) is actually the modal spring constant of the fundamental mode.

B. *Pull-in voltages*

To investigate the extraction of k from the pull-in voltage, C-V curves were measured on the four devices. Table 1 shows the extracted pull-in voltages of each device, as measured and according to the FEM model. The model reproduces the initial deformation effects and the resulting reduction in the pull-in voltage. Model and measurement results reflect the stable device behavior after the first two switching cycles. Comparing the results in table 1, the measured and modeled pull-in voltages differ by 1.5% to 7%. In other words, the FEM model matches the measurement quite well.

We use the pull-in voltage (of both FEM model and measurement) to calculate the spring constant, as further discussed in section III.D.

C. *Low-field capacitance method*

From the same C-V measurements we can obtain k also from the low-field capacitance. The low capacitance in the up-state is a complicating factor here, because the parabola method relies on the precise determination of small capacitance changes. In the device under test, both the minimum capacitance in the C-V curve and the open compensation are smaller than 1 pF and are in the lowest measurement range of the Keithley 4200 CVU, where the accuracy of the instrument is not specified in our version of the user manual.

Table 1 comparison of modeled and measured pull-in voltages.

V_{pi}	Device 3	Device 2	Device 1	Device 0
FEM model	20 V	44 V	49 V	52 V
Measurement	19.4V	44.7V	52.5V	54.7V

Indicative of the situation is the short term repeatability of the open compensation measurement. Figure 5 shows five consecutive measurements of an open structure, without any changes to the setup in between. Although each voltage sweep produces data with a very small rms value below 1% of the measured capacitance, which could be misinterpreted as an indication of a very accurate measurement, the consecutive sweeps yield results separated as much as 5% (sweeps 3 and 5).

This presumed drift is 0.031 pF which amounts to as much as 15% of the minimum capacitance of the MEMS switches under study. However, one may argue that the determination of the parabolic parameter a is rather insensitive to drift; so not all errors of the instrument will automatically affect the determination of k.

A second consideration in the determination of the spring constant from a is the chosen voltage range of the parabola measurement. If the range of DC bias is too large, the assumption that $u \ll g$ is imprecise. If the range of DC bias is too small, the C-V curve is noisy making the parabola fitting inaccurate. Figure 6 shows the relation between C/C_{min} and V_{DC} according to the FEM model. C_{min} is the minimum capacitance in the C-V curve. In the FEM model calculations for this article, dielectric charging was set to zero, so C_{min} in the FEM data is the capacitance at zero DC bias. The capacitance increases slowly with V_{DC} when the

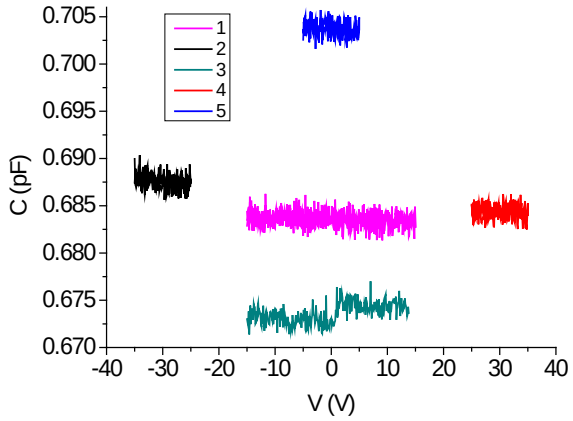

Figure 5: five consecutive measurements for the open compensation of device 3, indicating the short term repeatability.

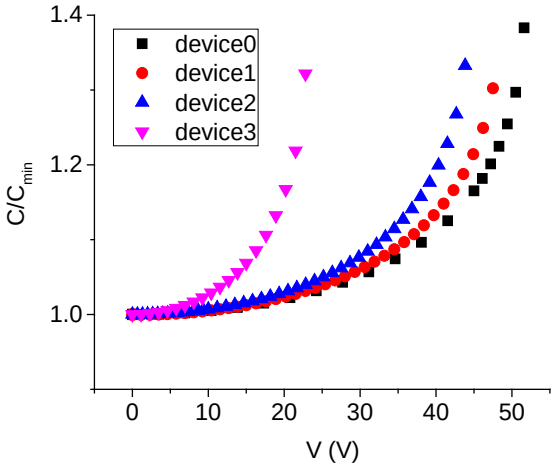

Figure 6: relation between C/C_{min} and V_{DC}, according to the FEM model.

DC bias is small; C increases dramatically when the DC bias approaches the pull-in voltage.

Figure 7 shows the outcome of the k-value obtained by the parabola method, for the 4 devices, and as calculated from FEM C-V data as well as measured C-V data. On the horizontal axis we plot the maximum value of the DC bias V_{DC} still included in the fit (so the fit is obtained on data from $-V_{DC}$ to $+V_{DC}$ in this figure). At lower DC bias ranges, the spring constant is correctly extracted, but at higher bias, the values are systematically off because of the deviation of C-V from the parabolic approximation (equation 6). When the DC bias range is chosen too low, erroneous values are obtained on the experimental data, as a result of measurement and calibration errors.

The k/k_3 from the measured low-field C-V curve is larger than the k/k_3 as obtained from modeled low-field C-V data. The reason is that in our analysis, we assumed the four devices under study to have the same air gap (as being determined by the thickness of the sacrificial layer in the fabrication process). However, the springs of fresh devices may have plastic deformation after the first several switching; so the air gap may change. This is particularly significant for the devices with short springs studied here, which were in fact designed for the purpose to quantify effects like this. The g in equation 7 may decrease because

of the plastic deformation. Device 3 has the longest springs, which almost have no plastic deformation. The shorter the springs are, the more significant the plastic deformation is. These effects can be quantitatively reproduced by the FEM model (not shown in this article). A more precise k determination than presented here can be achieved by establishing g separately for each device, for instance from the measured C_{min}.

In the further analysis we extract k values with this method using the following DC biases: 5 V, 15 V, 20 V and 20 V for device 3, device 2, device 1 and device 0 respectively.

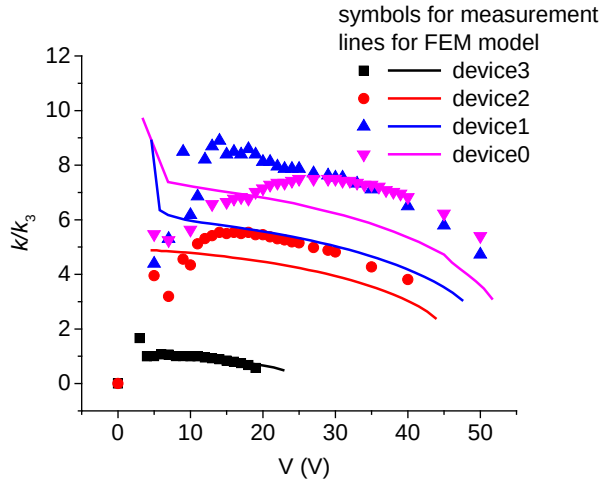

Figure 7: relation between normalized spring constant from low-field C-V parabola and the range of DC bias of the parabola, symbols for measurement and lines for FEM model; k_3 is the spring constant of device 3 calculated from the C-V parabola.

D. *Comparison of the three methods*

The spring constants calculated from the above three methods are shown in figure 8 and compared to the FEM result obtained from V_{pi}. As in figure 7, the results are normalized to the spring constant of device 3. All approaches yield a gradual increase of the spring constant when the springs are shorter, as expected; and quantitatively, a reasonable agreement is obtained. Only the k as obtained from the vibrometer deviates from the others. One possible reason is that the modal masses of the four devices are not accurately estimated with the weight of the plate.

We did find that the parabola method is very sensitive to the deviation of g and A, and depends on small differences between small capacitance values. Although the normalized k matches the FEM model well, we can hardly get an accurate absolute value of k from the parabola method.

V. Conclusions

We extracted the spring constant of four RF-MEMS capacitive switch designs using vibrometry, V_{pi}, and low-field C-V measurements. The obtained results were compared to a FEM model of the devices and the advantages and disadvantages of each method are described. The vibrometer results deviate from the other estimates, while we found that the low-field C-V method is relatively inaccurate due to measurement noise and parameter uncertainties.

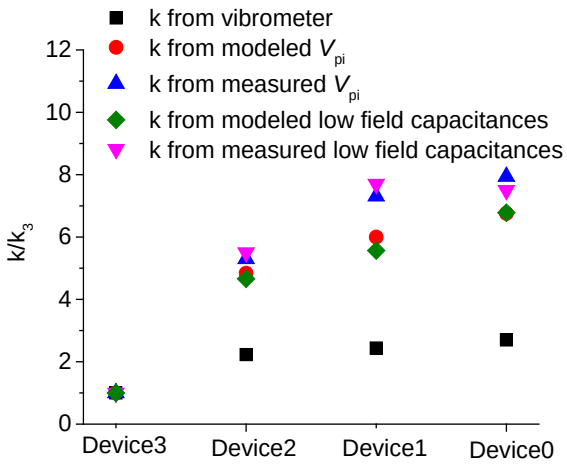

Figure 8: spring constants as obtained from three methods, normalized to the spring constant obtained on device3 (k_3).

Acknowledgements

This work has been performed in the EPAMO project, which is funded by public authorities of participant countries as well as by the ENIAC Joint Undertaking. We also would like to thank Remco G. P. Sanders and Sander M. Smits of the University of Twente for the help with our measurements, and Peter G. Steeneken of NXP Semiconductors and TU Delft for fruitful discussions.

References

[1] G. M. Rebeiz and J. B. Muldavin, “RF MEMS switches and switch circuit”, IEEE Microwave Magazine, vol. 2, issue 4, p. 67, 2001.

[2] S. J. Choi C.-H. Han, H.-H. Yang, D.-H. Choi, and J.-B. Yoon, “Increasing capacitance and self-resonant frequency of the MEMS switched capacitor using high-κ TiO_2 and SU-8 bridged beam structure”, Journal of Microelectromechanical Systems, vol. 24 issue 4, pp. 1006-1015, 2015.

[3] G. M. Rebeiz, “RF MEMS: theory, design and technology”, Wiley, 2003.

[4] J. Wang, C. Salm, and J. Schmitz, “Comparison of C-V measurement methods for RF-MEMS capacitive switches”, Proc. IEEE ICMTS conference 2013, pp. 53-58.

[5] M. Elwenspoek, G. Krijnen, R. Wiegerink, and T. Lammering, “Introduction to mechanics and transducer science”, textbook, University of Twente.

[6] R. W. Herfst, “Degradation of RF MEMS capacitive switches”, Ph.D. thesis, University of Twente, Enschede, The Netherlands 2008.

[7] J. Bielen, J. Stulemeijer, D. Ganjoo, and D. Ostergaard, “Efficient Multiphysics modeling of the dynamic response of RF-MEMS switches”, Proc. NAFEMS conference, North American Regional summit, 2008.

[8] J. Bielen, J. Stulemeijer, D. Ganjoo, D. Ostergaard and S. Noijen, “Fluid-electrostatic-mechanical modeling of the dynamic response of RF-MEMS capacitive switches”, Proc. IEEE EuroSimE 2008.

[9] M. Elwenspoek and R. Wiegerink, “Mechanical Microsensors”, 1st edition, Chapter 9, Springer 2001.

[10] R. W. Herfst, H. G. A. Huizing, P. G. Steeneken, and J. Schmitz, “Characterization of dielectric charging in RF MEMS capacitive switches”, Proc. IEEE ICMTS 2006, pp. 133-136.